JOURNAL OF VIROLOGY, Nov. 1981, p. 440-449
0022-538X/81/110440-10$02.00/0

Vol. 40, No. 2

Structures of the Oligosaccharides of the Glycoprotein Coded by Early Region E3 of Adenovirus 2

ROSALIND KORNFELD[1] AND WILLIAM S. M. WOLD[2]*

Division of Hematology and Oncology, Washington University School of Medicine,[1] and Institute for Molecular Virology, St. Louis University Medical Center,[2] St. Louis, Missouri 63110

Received 27 April 1981/Accepted 23 June 1981

Early region E3 of adenovirus 2 encodes a glycoprotein, E3-gp25K, that is a good model with which to study structure-function relationships in transmembrane glycoproteins. We have determined the structures of the oligosaccharides linked to E3-gp25K. The oligosaccharides were labeled with [2-^{3}H]mannose in adenovirus 2-early infected KB cells for 5.5 h (pulse) or for 5.5 h followed by a 3-h chase (pulse-chase). E3-gp25K was extracted and purified by chromatography on DEAE-Sephacel in 7 M urea, followed by gel filtration on a column of Bio-Gel A-1.5m in 6 M guanidine hydrochloride. An analysis of the purified protein by sodium dodecyl sulfate-polyacrylamide gel electrophoresis indicated that it was >95% pure. The oligosaccharides were isolated by pronase digestion followed by gel filtration on a column of Bio-Gel P-6, then by digestion with endo-β-*N*-acetylglucosaminidase H, followed by gel filtration on Bio-Gel P-6, and finally by paper chromatography. The pulse sample contained equal amounts of $Man_9GlcNAc$ and $Man_8GlcNAc$ and small amounts of $Man_7GlcNAc$ and $Man_6GlcNAc$. The pulse-chase sample had predominantly $Man_8GlcNAc$ and much less $Man_9GlcNAc$, indicating that processing of the $Man_9GlcNAc$ to $Man_8GlcNAc$ had occurred during the chase period. Thus, $Man_8GlcNAc$ is the major oligosaccharide on mature E3-gp25K. The structures of these oligosaccharides were established by digestion with α-mannosidase, methylation analysis, and acetolysis. The oligosaccharides found had typical high-mannose structures that have been observed in other membrane and soluble glycoproteins, and the branching patterns and linkages of the mannose residues of $Man_9GlcNAc$ were identical to those of the lipid-linked $Glc_3Man_9GlcNAc_2$ donor. Thus, adenovirus 2 infection (early stages) apparently does not affect the usual cellular high-mannose glycosylation pathways, and despite being virus coded, E3-gp25K is glycosylated in the same manner as a typical mammalian cell-coded glycoprotein.

Two glycoproteins, which we will designate E3-gp25K and E3-gp22K, are synthesized during early stages of infection of human cells by adenovirus 2 (Ad2) (9, 10, 20). (E3-gp25K and E3-gp22K have been referred to as E19K and E17.5K by other workers [19-21, 24-26]. We have used the designations gp25K and gp22K because they are glycoproteins that migrate in our sodium dodecyl sulfate [SDS]-gel system with apparent molecular weights of 25,000 [25K] and 22K, as judged by the relative mobilities of protein standards. Since glycoproteins generally migrate more slowly in SDS-gels than do non-glycosylated proteins of comparable molecular weight, the true molecular weights of E3-gp25K and E3-gp22K will be less than 25K and 22K.)

E3-gp25K and E3-gp22K have indistinguishable peptide maps and, thus, are highly related in their primary structures (19, 25; Q. Kapoor and W. Wold, unpublished data). Cells contain much more E3-gp25K than E3-gp22K. E3-gp25K is localized on the plasma membrane (4, 19, 20) and is complexed with the major transplantation antigen of the host cell (15). E3-gp25K has been purified to homogeneity, and antisera have been prepared (20; Kapoor and Wold, unpublished data).

Four lines of evidence prove that E3-gp25K is coded by early region E3 (map position 76 to 86). First, it is immunoprecipitated by antisera against Ad2-transformed cell lines that retain E3 (1, 10, 11, 23, 27). Second, it is not synthesized in cells infected by Ad2$^+$ND1, which has a deletion between map positions 80.3 and 85.5 (19, 24, 25). Third, it is translated in vitro from *r*-strand-specific and E3-specific mRNA (18, 19). Fourth,

the partial N-terminal amino acid sequence has been aligned with the DNA sequence in E3 (8, 19).

Aspects of the structure of gp25K can be predicted from the DNA sequence (8, 18). The primary translation product is 159 amino acids long, and it contains a putative N-terminal hydrophobic signal sequence of about 17 or 18 amino acids (18). The C-terminus contains a hydrophilic tail of 15 amino acids, which is preceded by a hydrophobic domain of 23 amino acids. There are two potential sites for N-glycosylation, Asn-Val-Thr, located in the N-terminal portion of the molecule. By analogy with other membrane glycoproteins that have a similar type of primary structure (21, 22), E3-gp25K may be oriented in the membrane such that the glycosylated N-terminal portion of the protein protrudes from the cell, the hydrophobic domain traverses the membrane, and the hydrophilic tail extends into the cytoplasm and anchors the protein in the membrane (18).

E3-gp25K was first shown to be glycosylated by labeling with [^{3}H]glucosamine (9, 10, 19, 20) or [2-^{3}H]mannose and by binding to concanavalin A or *Lens culinaris* lectins (10, 20). Glycosylation is inhibited by tunicamycin (19) or by 2-deoxyglucose or glucosamine (25). When translated in vitro, glycosylation occurs only in the presence of a microsomal fraction (18, 19).

Since much is known about E3-gp25K and since it is a viral gene product that is synthesized in fairly large amounts in infected cells, it is a good model with which to study structure-function relationships in transmembrane glycoproteins. In this communication, we report the complete structures of the oligosaccharides linked to E3-gp25K. The oligosaccharides, labeled with [2-^{3}H]mannose, were examined after a 5.5-h labeling period (pulse) and also after a 5.5-h labeling period followed by a 3-h chase (pulse-chase). At both times, all of the oligosaccharides were of the high-mannose type, with $Man_9GlcNAc_2$ and $Man_8GlcNAc_2$ predominating in the pulse sample and $Man_8GlcNAc_2$ predominating in the pulse-chase sample.

MATERIALS AND METHODS

Virus infection of cells and glycoprotein labeling. Methods used for the purification and quantitation of Ad2 stocks have been described previously (6, 28). Suspension cultures of KB cells were grown at 37°C at a concentration of 3.5×10^5 cells per ml in Eagle minimal essential medium (MEM) containing 5% horse serum. Cells from 2 liters were collected by centrifugation, suspended in 100 ml of MEM without horse serum, and infected with 500 PFU of Ad2 (strain 38-2) per cell. After 1 h, cells were diluted to 2 liters with MEM containing 5% horse serum. At 2.5 h postinfection, cells were collected by centrifugation and were washed in warm MEM containing 1/10 the normal glucose (i.e., 200 mg/liter) and 5% dialyzed horse serum. The washing step was repeated, and the cells were suspended in 1 liter of warm MEM containing 1/10 the normal glucose, 5% dialyzed horse serum, and 20 μg of 1-β-D-arabinofuranosylcytosine per ml. The 1-β-D-arabinofuranosylcytosine was used to inhibit the transition from early to late stages of infection, the resultant shutoff of E3-gp25K synthesis (20), and the possible modification of the host cell glycosylating machinery. At 3.5 h postinfection, 10 mCi of D-[2-^{3}H]mannose (New England Nuclear Corp.; 14.5 Ci/mmol) was added. Samples taken immediately after the addition of the label and at 1-h intervals indicated that incorporation of [2-^{3}H]mannose into trichloroacetic acid-insoluble material was linear over the labeling period (data not shown).

At 9 h postinfection, the cells were divided into two 500-ml lots, pulse and pulse-chase, and the cells were collected by centrifugation. The pulse-chase cells were washed once in warm MEM containing the normal amount of glucose, 5% horse serum, and 20 μg of 1-β-D-arabinofuranosylcytosine and then were further incubated in 500 ml of the same medium. The pulse cells were washed twice at 4°C with cold phosphate-buffered saline lacking Ca^{2+} and Mg^{2+} and then were kept on ice. At 12 h postinfection, the pulse-chase cells were collected and similarly washed with cold phosphate-buffered saline. Thus, both lots of cells were labeled for 5.5 h with [2-^{3}H]mannose, but the pulse-chase cells were chased for 3 h with glucose.

Extraction and purification of [2-^{3}H]mannose-labeled E3-gp25K. Cell pellets were suspended in 9 ml of isotonic high pH buffer (0.14 M NaCl, 1 mM $MgCl_2$, 10 mM Tris-hydrochloride, pH 8.5) containing 1 mM phenylmethylsulfonyl fluoride (a protease inhibitor) at 1 to 2°C and were lysed by the addition of Nonidet P-40 to a concentration of 0.5%. After 5 min of gentle mixing with a pipette, the nuclei were removed by centrifugation at $200 \times g$ for 10 min at 4°C. The supernatant was removed, and the pellet was washed once with lysis buffer. The supernatants were pooled and clarified by centrifugation at $12,000 \times g$ for 10 min at 4°C in a Sorvall SS-34 rotor and then at $82,000 \times g$ for 1 h at 4°C in a 50 Ti rotor. Triton X-100 was added to a final concentration of 1%, and the samples were dialyzed for 2 days at 4°C against DEAE buffer (6 M urea, 10 mM NaCl, 1% Triton X-100, 1 mM dithiothreitol, 1 mM phenylmethylsulfonyl fluoride, 20 mM Tris-hydrochloride, pH 8.5). The yield at this stage was 1.38×10^8 and 8.27×10^7 cpm for the pulse and pulse-chase samples, respectively.

Two DEAE-Sephacel columns (1.1 by 7 cm) were poured, equilibrated against DEAE buffer, and loaded with the protein samples at a rate of 3 ml/h. The columns were washed with DEAE buffer until the counts being eluted were negligible and then were eluted with DEAE buffer containing 1 M NaCl. The two flow-through pools and the two 1 M NaCl eluate pools were dialyzed at 4°C for 2 days against several changes of 50 mM NH_4HCO_3–0.01% Triton X-100. An analysis of the fractions by polyacrylamide gel electrophoresis in SDS (SDS-PAGE) indicated that most of the E3-gp25K was in the flow-through fractions, but

that it was contaminated by a number of cellular glycoproteins. The pulse and pulse-chase flow-through fractions contained 2.2×10^7 and 1.2×10^7 cpm, respectively.

E3-gp25K was further purified by gel filtration, as follows. The dialyzed DEAE flow-through fractions were lyophilized, suspended in about 5 ml of 0.4 M glycine, mixed with 5 volumes of cold acetone, and precipitated for 2 h at 0 to 2°C. The proteins coprecipitated with the large flocculent glycine precipitate that formed in the presence of acetone. The acetone extracts the Triton X-100 (at a high concentration after the lyophilization step), which must be removed because it forms micelles which preclude partitioning of proteins in the gel filtration column. The glycine-protein pellets were suspended in 50 mM NH_4HCO_3–0.01% Triton X-100, lyophilized, and resuspended in 0.7 ml of 8 M guanidine hydrochloride–2% 2-mercaptoethanol–10 mM EDTA–50 mM Tris-hydrochloride, pH 8.5. The recovery of counts was >95%. The samples were heated at 56°C for 45 min to dissociate the polypeptides and were neutralized with 0.1 ml of 1 M sodium phosphate, pH 6.5. The samples were mixed with a small volume of phenol red containing 100 mg of sucrose and were applied to a column (1.5 by 100 cm) of Bio-Gel A-1.5m equilibrated in 6 M guanidine hydrochloride–10 mM dithiothreitol–1 mM phenylmethylsulfonyl fluoride–20 mM sodium phosphate buffer, pH 6.5. One-hour (3.5-ml) fractions were collected. All fractions were adjusted to 0.02% Triton X-100 and were dialyzed against 50 mM NH_4HCO_3–0.02% Triton X-100. Each fraction was counted, and selected fractions were assayed by SDS-PAGE, using the deoxycholate-trichloroacetic acid precipitation method (see below).

SDS-PAGE. SDS-PAGE was carried out with discontinuous 13% polyacrylamide gels as described previously (27). Triton X-100 causes "smearing" on gels; therefore, it was extracted from the protein samples before SDS-PAGE, as described below. The samples, adjusted to 0.5 ml in 1.5-ml Eppendorf tubes, were mixed (Vortex) with 10 μl of 2% sodium deoxycholate and incubated at room temperature for 15 min. Trichloroacetic acid was added to a final concentration of 10%, and the samples were incubated at 0 to 2°C for 30 min. The heavy trichloroacetic acid-deoxycholate-protein precipitate that formed was removed by centrifugation for 4 min in an Eppendorf microfuge. The pellets were washed twice with 1 ml of cold acetone and finally were suspended in 20 to 50 μl of SDS-PAGE sample buffer (27).

Preparation of labeled glycopeptides. The retained fractions of the Bio-Gel A-1.5m column that contained purified E3-gp25K (see Fig. 1) were pooled and lyophilized. Each pool was dissolved in 1.5 ml of water and extracted twice with 2 ml of toluene to remove Triton X-100. The somewhat turbid solutions were incubated at 60°C with 7 mg of pronase in 2 mM $CaCl_2$–0.1 M Tris-hydrochloride, pH 8.0. After 4 h, an additional 7 mg of pronase was added. After 20 h, each reaction was boiled for 2 min and subjected to gel filtration on a column (1.5 by 98 cm) of Bio-Gel P-6 to isolate the glycopeptides (see Fig. 2 below).

Preparation of oligosaccharides. The glycopeptide fractions from each sample, obtained from the Bio-Gel P-6 column, were lyophilized and redissolved in 2.5 ml of water. One milliliter of each glycopeptide sample was taken to dryness and incubated for 19 h at 37°C in 100 μl of 50 mM citrate phosphate buffer, pH 6.5, containing 2 mU of endo-β-*N*-acetylglucosaminidase H (endo H) (Miles Laboratories, Inc.). The samples, diluted to 1.0 ml with water, were boiled for 3 min and again subjected to gel filtration on Bio-Gel P-6 as shown in Fig. 2. The pooled oligosaccharide fractions from the Bio-Gel P-6 column were lyophilized, redissolved in water, spotted on Whatman no. 1 paper, and subjected to descending paper chromatography in pyridine-ethyl acetate-acetic acid-water (5:5:1:3), solvent I, for 7 days to separate oligosaccharides according to size. The sample lanes and a lane containing oligosaccharide standards of known size were cut in 1-cm segments which were eluted in 1.0 ml of water. A sample of each was counted, and eluates were pooled that corresponded to $Man_9GlcNAc$, $Man_8GlcNAc$, $Man_7GlcNAc$, and $Man_6GlcNAc$ (see Fig. 3).

Structural analysis of oligosaccharides. The oligosaccharides were methylated by the method of Hakomori (7), and the permethylated products were hydrolyzed in 2 N H_2SO_4 and analyzed by thin-layer chromatography as reported by Li et al. (16). Labeled oligosaccharides were reduced with $NaBH_4$ and subjected to acetolysis as previously described (2). The Man → Man disaccharides obtained by acetolysis were reduced with $NaBH_4$ and subjected to molybdate electrophoresis as previously described (2) to separate Man $\xrightarrow{\alpha 1,2}$ mannitol from Man $\xrightarrow{\alpha 1,3}$ mannitol. Oligosaccharides were digested with jack bean α-mannosidase prepared by the method of Li and Li (17) by incubation at 37°C with 1 U of enzyme in 20 μl of 50 mM acetate buffer, pH 4.6, for 1.5 h. The digestions were then subjected to descending chromatography on Whatman no. 1 paper in solvent I for 16 h to separate free mannose from Man → GlcNAc disaccharide.

RESULTS

Purity of [2-^{3}H]mannose-labeled E3-gp25K. Figure 1A shows the Bio-Gel A-1.5m column elution profile of the labeled glycoproteins from the pulse-labeled cells. Fractions 20, 33, 34, 35, 36, and 37–41 pool were analyzed by SDS-PAGE. The majority of E3-gp25K was found in the major retained peak, fractions 33 to ~37 (Fig. 1B). Some E3-gp25K was also found in the void volume, despite the use of 6 M guanidine hydrochloride and 10 mM dithiothreitol in the column buffer, which attests to the tendency of this polypeptide to aggregate. A small quantity of E3-gp22K was found in fractions 35 to 41. The 44K glycopolypeptide in fractions 34 to 36 is highly related to E3-gp25K, because it has a very similar [^{35}S]methionine-containing peptide map (27; Q. Kapoor and W. Wold, unpublished data). The apparent molecular weight estimate of 44K for this glycopolypeptide does not rule out the possibility that it is a dimer of gp25K, because the mobility of

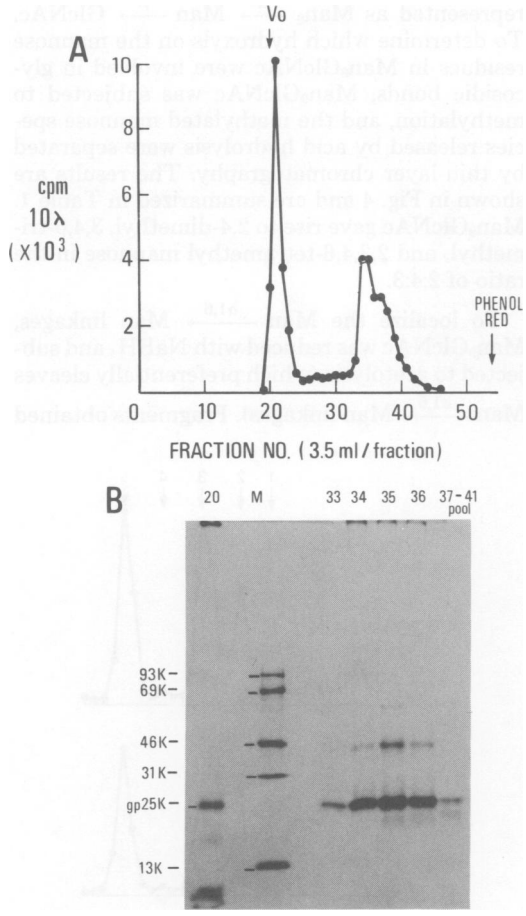

FIG. 1. *Gel filtration of [2-³H]mannose pulse-labeled E3-gp25K on a column of Bio-Gel A-1.5m. The column was prepared and run as described in the text. (A) Elution profile of the labeled glycopolypeptides. (B) SDS-protein gel which illustrates the glycopolypeptides in fractions 20, 33, 34, 35, 36, and 37-41 pool. "M" refers to ¹⁴C-labeled protein standards (New England Nuclear Corp.), which were phosphorylase b (93K), bovine serum albumin (69K), ovalbumin (46K), carbonic anhydrase (31K), and cytochrome c (13K).*

glycopolypeptides in SDS-gels is not an accurate indication of their molecular weights. The 60K glycopolypeptide in fraction 35 may have been yet another form (e.g., trimer) of E3-gp25K or it may have been a contaminant. If it was a contaminant, its concentration was much too low to compromise our analysis of the oligosaccharides of E3-gp25K. Similar results were obtained with the glycoproteins from the pulse-chase-labeled sample (data not shown). Fractions 33 to 41 in Fig. 1 were pooled, as were analogous fractions from the pulse-chase-labeled sample, and the glycopeptides were prepared by pronase digestion.

Purification of the oligosaccharides of E3-gp25K. Figure 2 shows the Bio-Gel P-6 column profile of the glycopeptides obtained on the pronase digest of the pulse-labeled sample (solid line) and on the oligosaccharides released from these glycopeptides by endo H digestion (dashed line). Essentially the same profile was obtained for the pulse-chase sample. Endo H cleaves the two *N*-acetylglucosamine residues of the chitobiose core of high-mannose, asparagine-linked oligosaccharides, liberating an oligosaccharide with one *N*-acetylglucosamine residue at its reducing end and leaving one *N*-acetylglucosamine residue attached to asparagine in the peptide. Kobata (12) has recently reviewed the specificity studies that show that endo H can act on high-mannose oligosaccharides, but not on the complex type. In both the pulse and pulse-chase samples, all of the [2-³H]mannose-labeled oligosaccharides were susceptible to endo H cleavage and thus must be of the high-mannose-type structure.

The oligosaccharide fractions from the Bio-Gel P-6 columns were subjected to paper chromatography to resolve the different sized oligosaccharides. The pulse sample contained almost equal amounts of oligosaccharides comigrating with authentic $Man_9GlcNAc$ (nine mannose residues linked to *N*-acetylglucosamine) and $Man_8GlcNAc$, as well as much smaller amounts

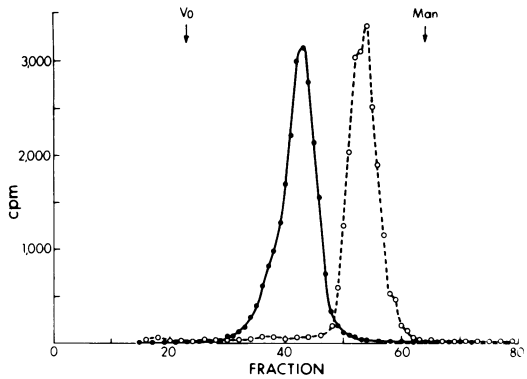

FIG. 2. *Bio-Gel P-6 gel filtration of the glycopeptides in the pronase digest (●) and the oligosaccharides released from them after endo H digestion (○). The Bio-Gel P-6 column (1.5 by 98 cm) was equilibrated and eluted with 0.1 M ammonium bicarbonate, and 2-ml fractions were collected. Samples of every fraction were counted in a solution containing 4 ml of 3a70 scintillation fluid and 0.4 ml of water. Fractions 32 to 50 were pooled from the glycopeptide peak, and fractions 49 to 60 were pooled from the oligosaccharide peak.*

of material comigrating with $Man_7GlcNAc$ and $Man_6GlcNAc$ (Fig. 3A). In contrast, the pulse-chase sample (Fig. 3B) contained predominantly $Man_8GlcNAc$, with much less $Man_9GlcNAc$. Upon rechromatography, each of the pooled eluates from the first separation migrated as single peaks coincident with $Man_{9-6}GlcNAc$ standards. The quantitative difference in $Man_9GlcNAc$ between the pulse and the pulse-chase samples indicated that processing of the oligosaccharide to its mature form had occurred during the chase period.

Structural studies on each oligosaccharide species from both the pulse and pulse-chase samples were performed as described below, but data are shown only for the pulse samples. Results were essentially identical for the pulse-chase sample oligosaccharides.

Structure of the $Man_9GlcNAc$ oligosaccharide. When the oligosaccharide with the same mobility as $Man_9GlcNAc$ was digested with α-mannosidase, 89% of the radioactivity migrated upon paper chromatography as free mannose and 11% migrated as the disaccharide Man $\xrightarrow{\beta 1,4}$ GlcNAc (data not shown). Thus, it contained eight α-mannose residues and can be represented as $Man_8 \xrightarrow{\alpha}$ Man $\xrightarrow{\beta}$ GlcNAc. To determine which hydroxyls on the mannose residues in $Man_9GlcNAc$ were involved in glycosidic bonds, $Man_9GlcNAc$ was subjected to methylation, and the methylated mannose species released by acid hydrolysis were separated by thin-layer chromatography. The results are shown in Fig. 4 and are summarized in Table 1. $Man_9GlcNAc$ gave rise to 2,4-dimethyl, 3,4,6-trimethyl, and 2,3,4,6-tetramethyl mannose in the ratio of 2:4:3.

To localize the Man $\xrightarrow{\alpha 1,6}$ Man linkages, $Man_9GlcNAc$ was reduced with $NaBH_4$ and subjected to acetolysis (which preferentially cleaves Man $\xrightarrow{\alpha 1,6}$ Man linkages). Fragments obtained

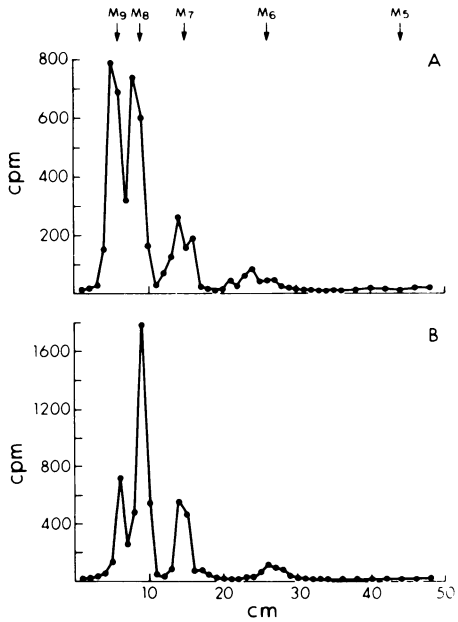

FIG. 3. *Preparative paper chromatography of oligosaccharides released by digestion with endo H. The chromatograms were developed and analyzed as described in the text. (A) Pulse sample; (B) pulse-chase sample. The arrows show the migration positions of authentic $Man_9GlcNAc$-$Man_5GlcNAc$ oligosaccharides. Fractions corresponding to each peak were pooled and analyzed further.*

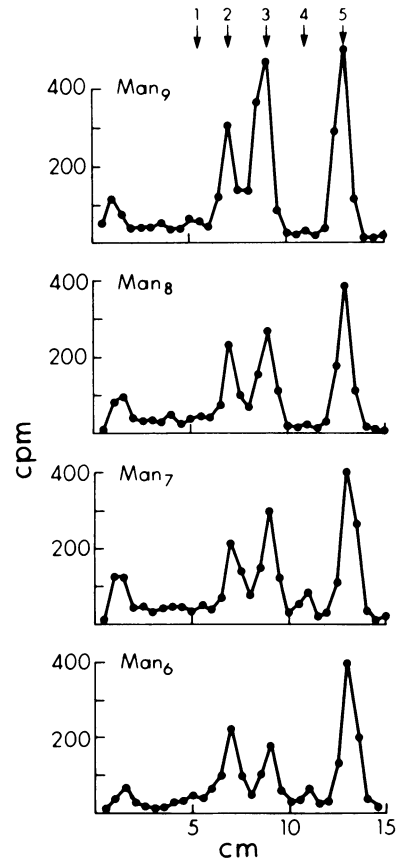

FIG. 4. *Thin-layer chromatography of the methylated mannose species derived from the pooled oligosaccharide fractions shown in Fig. 3. The thin-layer plates were developed and analyzed as described in the text. The arrows at the top denote the migration positions of the following authentic methylated mannose species: (1) 2,3-dimethyl, (2) 2,4-dimethyl, (3) 3,4,6-trimethyl; (4) 2,4,6-trimethyl, and (5) 2,3,4,6-tetramethyl mannose.*

TABLE 1. *Methylation of pulse-labeled oligosaccharides and acetolysis fragments*

Sample	No. of mannose residues[a]			
	2,3,4,6-Tetramethyl mannose	2,4,6-Trimethyl mannose	3,4,6-Trimethyl-mannose	2,4-Dimethyl mannose
Intact oligosaccharides				
$Man_9GlcNAc$	3.2	0	3.8	2.0
$Man_8GlcNAc$	3.2	0	2.9	1.9
$Man_7GlcNAc$	2.8	0.4	2.1	1.7
$Man_6GlcNAc$	2.8	0.2	1.2	1.8
Acetolysis fragments of $Man_9GlcNAc$				
Man → Man → Man	1.1	0.9	1.0	0
$Man_4GlcitolNAc$	1.1	0.9	2.0	0

[a] The sum of the radioactivity in all species of methylated mannose in each sample in Fig. 4 was set equal to the number of mannose residues in that sample and the counts per minute per mannose residue were calculated for each sample. This value was then used to determine the number of mannose residues of every methylated species.

had the same mobilities as authentic $Man_4GlcitolNAc$, Man_3, and Man_2 (Fig. 5A). These results suggested the structure shown in Fig. 5A, where the dashed lines indicate cleavage sites at α1,6 linkages. The two larger fragments were characterized further by methylation (Table 1). Man_2 was shown to be linked α1,2 by subjecting the material to $NaBH_4$ reduction followed by high-voltage electrophoresis in molybdate buffer, which separates Man $\xrightarrow{\alpha 1,2}$ mannitol from Man $\xrightarrow{\alpha 1,3}$ mannitol (data not shown).

The results establish that $Man_9GlcNAc$ contains two branching mannose residues substituted at C-3 and C-6, giving rise to 2,4-dimethyl mannose after methylation, which must be linked to one another via an α1,6 linkage as shown in Fig. 5A to produce the fragments observed upon acetolysis. The Man_3 fragment contains one terminal mannose residue (giving rise to 2,3,4,6-tetramethyl mannose), one residue substituted at C-2 (giving rise to 3,4,6-trimethyl mannose), and one residue substituted at C-3 (giving rise to 2,4,6-trimethyl mannose) which must have originally been one of the branch point mannose residues. The other original branch point mannose is in the $Man_4GlcitolNAc$ fragment, where it is substituted at C-3 (giving rise to 2,4,6-trimethyl mannose). Also present in this fragment are one terminal mannose residue and two mannose residues substituted at C-2. These results provide evidence that the $Man_9GlcNAc$ has the structure shown in Fig. 6.

Structure of the $Man_8GlcNAc$ oligosaccharide. When the $Man_8GlcNAc$ oligosaccharide was digested with α-mannosidase, 88% of the radioactivity was released as free mannose, and 12% had the chromatographic mobility of Man $\xrightarrow{\beta 1,4}$ GlcNAc, indicating the presence of seven α-mannose residues. As indicated in Fig. 4 and Table 1, methylation of the oligosaccharide gave rise to 2,4-dimethyl, 3,4,6-trimethyl and 2,3,4,6-tetramethyl mannose in the ratio of

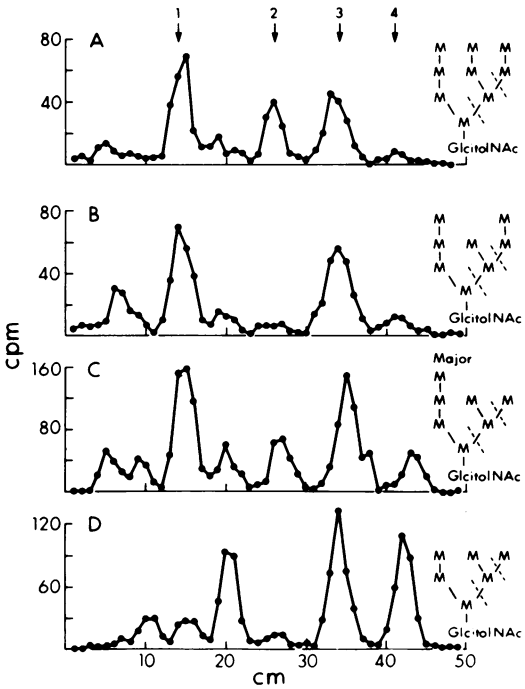

FIG. 5. *Paper chromatography of the fragments produced by acetolysis of the oligosaccharides. The structures at the right indicate the structures deduced from the data, with the dashed lines showing the location of the α1,6 linkages that are preferentially cleaved by acetolysis. (A) $Man_9GlcNAc$, (B) $Man_8GlcNAc$, (C) $Man_7GlcNAc$, and (D) $Man_6GlcNAc$. The arrows at the top denote the migration positions of the following standard oligosaccharides: (1) $Man_4GlcitolNAc$, (2) Man_3, (3) Man_2, and (4) mannose.*

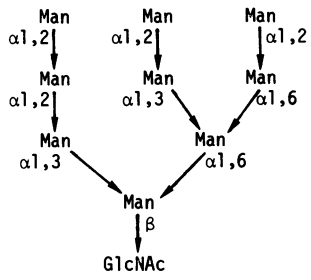

$Man_9GlcNAc$

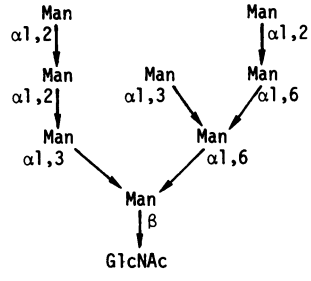

$Man_8GlcNAc$

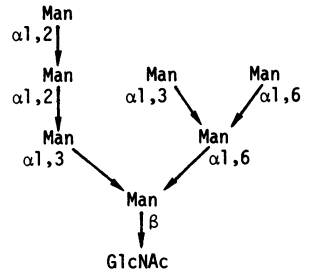

A (major)

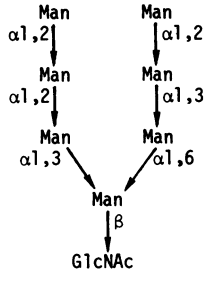

B

(minor)

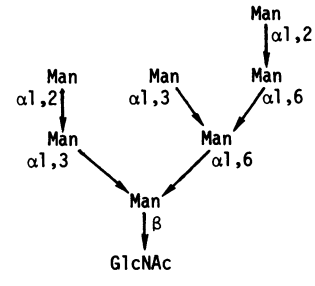

C

$Man_7GlcNAc$

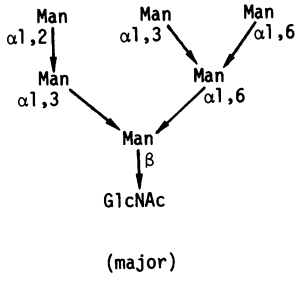

(major)

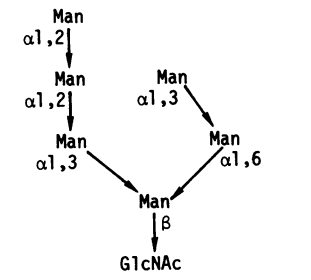

(minor)

$Man_6GlcNAc$

FIG. 6. *Structures proposed for the oligosaccharides of E3-gp25K.*

2:3:3. Acetolysis of $Man_8GlcNAc$ produced two major fragments corresponding to Man_4-GlcitolNAc and Man_2 (Fig. 5B). Molybdate electrophoresis (data not shown) resolved the reduced Man_2 into two peaks, one comigrating with Man $\xrightarrow{\alpha 1,2}$ mannitol and the other comigrating with Man $\xrightarrow{\alpha 1,3}$ mannitol in the ratio of 1.5:1.0. The structure expected to yield these fragments is shown in Fig. 5B and Fig. 6. The excess Man $\xrightarrow{\alpha 1,2}$ mannitol obtained probably reflects some underdegradation in the acetolysis reaction, in which only a single cleavage occurred, giving rise to Man $\xrightarrow{\alpha 1,2}$ Man and $Man_6GlcitolNAc$. The latter would account for the slowest-moving peak on the chromatogram in Fig. 5B. The methylation and acetolysis data indicate that $Man_8GlcNAc$ has the structure proposed in Fig. 6.

Structure of the $Man_7GlcNAc$ oligosaccharide. When $Man_7GlcNAc$ was treated with α-mannosidase, 85% of the radioactivity was released as free mannose and 15% comigrated with Man $\xrightarrow{\beta 1,4}$ GlcNAc disaccharide, indicating the presence of six α-mannose residues. The methylation products shown in Fig. 4 and Table 1 and the acetolysis cleavage pattern shown in Fig. 5C both indicate the presence of more than one isomeric $Man_7GlcNAc$ structure in this oligosaccharide. Acetolysis produced major fragments corresponding to $Man_4GlcitolNAc$, Man_2, and free mannose; this is consistent with the structure and cleavage sites shown in Fig. 5C for the major $Man_7GlcNAc$ species. However, significant amounts of fragments corresponding to $Man_3GlcitolNAc$ and Man_3 were also produced, and molybdate electrophoresis revealed that the Man_2 contained both Man $\xrightarrow{\alpha 1,3}$ Man (expected from the major species) and Man $\xrightarrow{\alpha 1,2}$ Man. To account for the Man_3 fragment and for the production of 2,4,6-trimethyl mannose and less than two full residues of 2,4-dimethyl mannose from $Man_7GlcNAc$, we propose that a minor species with the B structure occurs along with the major A structure (Fig. 6). To account for the $Man_3GlcitolNAc$ fragment and the Mn $\xrightarrow{\alpha 1,2}$ Man fragment, we also propose that another minor species with the C structure shown in Fig. 6 also occurs in $Man_7GlcNAc$.

Structure of the $Man_6GlcNAc$ oligosaccharide. When the $Man_6GlcNAc$ was treated with α-mannosidase, 84% of the radioactivity was released as free mannose and 16% migrated with Man $\xrightarrow{\beta 1,4}$ GlcNAc. This indicates five α-mannose residues. Methylation of $Man_6GlcNAc$ gave the results shown in Fig. 4 and Table 1, and acetolysis produced the fragmentation pattern shown in Fig. 5D. The fragments corresponded to $Man_3GlcitolNAc$, Man_2, and free mannose and fit the structure with the cleavage sites shown in Fig. 5D. All of the Man_2 was shown to be Man $\xrightarrow{\alpha 1,3}$ Man by molybdate electrophoresis; thus, the structure of the vast majority of the $Man_6GlcNAc$ oligosaccharide must be as shown in Fig. 6 for the major species. This oligosaccharide should give rise to 2,4-dimethyl, 3,4,6-trimethyl, and 2,3,4,6-tetramethyl mannose in the ratio 2:1:3 and produce no 2,4,6-trimethyl mannose. In fact, the methylation results (Table 1) indicate the presence of 0.2 residue of 2,4,6-trimethyl mannose, 0.2 residue more 3,4,6-trimethyl mannose than expected, and 0.2 residue less 2,4-dimethyl and tetramethyl mannose than expected; this suggests that 20% of $Man_6GlcNAc$ has the structure shown in Fig. 6 as the minor species. This structure would produce a $Man_4GlcitolNAc$ fragment upon acetolysis, and inspection of Fig. 5D shows a small radioactive peak at that position.

DISCUSSION

Glycosylation of proteins in mammalian cells occurs by en bloc transfer of a $Glc_3Man_9GlcNAc_2$ moiety from a lipid-linked oligosaccharide donor (16). Typically, the various types of high-mannose and complex oligosaccharides found on glycoproteins are generated by processing of $Glc_3Man_9GlcNAc_2$ as the newly synthesized glycoproteins travel from the rough endoplasmic reticulum through the Golgi region, with removal of the three glucoses occurring very rapidly (14). In our analyses of the oligosaccharides released by endo H, we found that the pulse-labeled sample, which should contain newly synthesized and mature E3-gp25K, gave rise to equal amounts of $Man_9GlcNAc$ and $Man_8GlcNAc$ and much smaller amounts of $Man_7GlcNAc$ and $Man_6GlcNAc$. In contrast, the pulse-chase-labeled sample, which should contain only mature E3-gp25K, gave rise to mainly $Man_8GlcNAc$, with considerably less $Man_9GlcNAc$, $Man_7GlcNAc$, and $Man_6GlcNAc$. This implies that $Man_9GlcNAc$ was processed mainly into $Man_8GlcNAc$ during the 3-h chase period. The branching pattern and linkage of the mannose residues that we found in the $Man_9GlcNAc$ oligosaccharide from E3-gp25K are identical to those in the lipid-linked $Glc_3Man_9GlcNAc_2$ previously described (16), suggesting that E3-gp25K is initially glycosylated by this precursor oligosaccharide and then three glucose residues are trimmed off.

In the case of glycoproteins having high-mannose oligosaccharides smaller than $Man_9GlcNAc_2$, there is generally some degree of heterogeneity in the number of mannose residues introduced during the processing reactions catalyzed by the Golgi α1,2-mannosidase (26). This type of size heterogeneity has been described for the heavy-chain oligosaccharides of human immunoglobulin M myeloma proteins (2, 3, 5), and in the present study, this mechanism probably accounts for the small amounts of $Man_7GlcNAc$ and $Man_6GlcNAc$ species observed. In addition to size heterogeneity, high-mannose oligosaccharides can display structural heterogeneity among oligosaccharides of the same size. Although three possible $Man_8GlcNAc$ oligosaccharide isomers can be formed by the cleavage of a single terminal mannose residue from $Man_9GlcNAc$, we found only one isomer, indicating that the removal of the first mannose residue from the

E3-gp25K oligosaccharide is specific and not random. A similar finding has been made for several other glycoproteins (3, 5). However, since several $Man_7GlcNAc$ isomers and two $Man_6GlcNAc$ isomers were found, the subsequent mannose processing was either less ordered, or different patterns of ordered removal occurred at separate glycosylation sites to generate these smaller, quantitatively minor species. The oligosaccharides of E3-gp25K are all typical high-mannose oligosaccharides having structures identical to those found in a variety of other membrane and soluble glycoproteins (13). Other viral glycoproteins, for example, the G protein of vesicular stomatitis virus (14), are initially glycosylated by the host cell with a high-mannose oligosaccharide, which is then processed and converted to a complex-type oligosaccharide by the addition of outer chain *N*-acetylglucosamine, galactose, and sialic acid residues and by the addition of fucose to the core *N*-acetylglucosamine. In the case of E3-gp25K, we found no evidence that such complex chains were formed, as shown by the fact that the oligosaccharides were quantitatively cleaved by endo H and could be degraded completely to Man $\xrightarrow{\beta}$ GlcNAc by treatment with α-mannosidase. The factors that determine whether the oligosaccharide at a given glycosylation site on a particular protein will remain a high-mannose type or be converted to a complex type by glycosyl transferases of the Golgi apparatus are not known, but probably the conformation of the polypeptide is one factor.

The DNA sequence of the putative gene for E3-gp25K reveals two potential sites for Asn-linked glycosylation (8, 19). Although there are no direct data, circumstantial evidence suggests that both sites may be glycosylated. For example, Persson et al. (20) found 4 mol of *N*-acetylglucosamine per mol of E3-gp25K, which is consistent with 2 mol of $Man_8GlcNAc_2$. Further, the apparent molecular weight of nonglycosylated gp25K, obtained by infecting cells in the presence of tunicamycin (19, 20) or by cleaving with endo H (Q. S. Kapoor, W. S. M. Wold, and G. Chinnadurai, Virology, in press), is about 4.5K to 6K smaller than glycosylated gp25K as estimated by SDS-PAGE. Only 1 mol of $Man_8GlcNAc_2$, with a molecular weight of 1.7K, is unlikely to cause such a large difference. If there are, in fact, 2 mol of the same $Man_8GlcNAc_2$ moiety per mol of gp25K and if they are linked to the two Asn-Val-Thr sites predicted by the DNA sequence, it is of interest that there are no obvious similarities in the amino acids proximal to these sites (8, 19). Thus, the signals that dictate the oligosaccharide structure at a given glycosylation site are not obvious from a casual inspection of the amino acid sequence of the glycosylation sites; perhaps these signals are degenerate, or perhaps they involve protein folding.

ACKNOWLEDGMENTS

We thank Maurice Green for support and for reading the manuscript and Catherine Devine and Karen Fujimoto for excellent technical assistance.

This work was supported by Public Health Service research grants CA-24710 and CA-08759 and Cancer Center Core grant CA-25843 from the National Institutes of Health. W.S.M.W. was supported by Public Health Service Research Career Development award CA-00650 from the National Institutes of Health.

LITERATURE CITED

1. **Brackmann, K. H., M. Green, W. S. M. Wold, and M. Cartas.** 1980. Identification and peptide mapping of adenovirus 2-induced early polypeptides isolated by two dimensional gel electrophoresis. J. Biol. Chem. **255:** 6772–6779.
2. **Chapman, A., and R. Kornfeld.** 1979. Structure of the high mannose oligosaccharides of a human IgM myeloma protein. I. The major oligosaccharides of the two high mannose glycopeptides. J. Biol. Chem. **254:**816–823.
3. **Chapman, A., and R. Kornfeld.** 1979. Structure of the high mannose oligosaccharides of a human IgM myeloma protein. II. The minor oligosaccharides of high mannose glycopeptide I. J. Biol. Chem. **254:**824–828.
4. **Chin, W. W., and J. V. Maizel, Jr.** 1976. Polypeptides of adenovirus. VII. Further studies of early polypeptides *in vivo* and localization of E2 and E2A to the cell plasma membrane. Virology **71:**518–530.
5. **Cohen, R. E., and C. E. Ballou.** 1980. Linkage and sequence analysis of mannose-rich glycoprotein core oligosaccharides by proton nuclear magnetic resonance spectroscopy. Biochemistry **19:**4345–4358.
6. **Green, M., and W. S. M. Wold.** 1979. Preparation of human adenoviruses. Methods Enzymol. **58:**425–435.
7. **Hakomori, S.** 1974. A rapid permethylation of glycolipid and polysaccharide catalyzed by methylsulfinyl carbanion in dimethyl sulfoxide. J. Biochem. (Toyko) **55:** 205–208.
8. **Hérissé, J., G. Courtois, and F. Galibert.** 1980. Nucleotide sequence of the EcoRI D fragment of adenovirus 2 genome. Nucleic Acids Res. **8:**2173–2192.
9. **Ishibashi, M., and J. V. Maizel, Jr.** 1974. The polypeptides of adenoviruses. VI. Early and late glycopolypeptides. Virology **58:**345–361.
10. **Jeng, Y-H., W. S. M. Wold, and M. Green.** 1978. Evidence for an adenovirus type 2-coded early glycoprotein. J. Virol. **28:**314–323.
11. **Johansson, K., H. Persson, A. M. Lewis, U. Pettersson, C. Tibbetts, and L. Philipson.** 1978. Viral DNA sequences and gene products in hamster cells transformed by adenovirus type 2. J. Virol. **27:**628–639.
12. **Kobata, A.** 1979. Use of endo- and exoglycosidases for structural studies of glycoconjugates. Anal. Biochem. **100:**1–14.
13. **Kornfeld, R., and S. Kornfeld.** 1980. Structure of glycoproteins and their oligosaccharide units, p. 1–34. *In* W. J. Lennarz (ed.), The biochemistry of glycoproteins and proteoglycans. Plenum Publishing Corp., New York.
14. **Kornfeld, S., E. Li, and I. Tabas.** 1978. The synthesis of complex-type oligosaccharides. II. Characterization of the processing intermediates in the synthesis of the complex oligosaccharide units of the vesicular stomati-

tis virus G protein. J. Biol. Chem. **253**:7771–7778.

15. **Kvist, S., L. Östberg, H. Persson, L. Philipson, and P. A. Peterson.** 1978. Molecular association between transplantation antigens and cell surface antigen in adenovirus-transformed cell line. Proc. Natl. Acad. Sci. U.S.A. **75**:5674–5678.
16. **Li, E., I. Tabas, and S. Kornfeld.** 1978. The synthesis of complex-type oligosaccharides. I. Structure of the lipid-linked oligosaccharide precursor of the complex-type oligosaccharides of the vesicular stomatitis virus G protein. J. Biol. Chem. **253**:7762–7770.
17. **Li, Y. T., and S. C. Li.** 1972. α-Mannosidase, β-*N*-acetyl hexosaminidase, and β-galactosidase from Jack Bean Meal. Methods Enzymol. **28**:702–713.
18. **Persson, H., M. Jansson, and L. Philipson.** 1980. Synthesis and genomic site for an adenovirus type 2 early glycoprotein. J. Mol. Biol. **136**:375–394.
19. **Persson, H., H. Jörnvall, and J. Zabielski.** 1980. Multiple mRNA species for the precursor to an adenovirus-encoded glycoprotein: identification and structure of the signal sequence. Proc. Natl. Acad. Sci. U.S.A. **77**: 6349–6353.
20. **Persson, H., C. Signäs, and L. Philipson.** 1979. Purification and characterization of an early glycoprotein from adenovirus type 2-infected cells. J. Virol. **29**:938–948.
21. **Rogers, J., P. Early, C. Carter, K. Calamine, M. Bond, L. Hood, and R. Wall.** 1980. Two mRNAs with different 3′ ends encode membrane-bound and secreted forms of immunoglubulin μ chain. Cell **20**:303–312.
22. **Rose, J. K., W. J. Welch, B. M. Sefton, F. S. Esch, and N. C. Ling.** 1980. Vesicular stomatitis virus glycoprotein is anchored in the viral membrane by a hydrophobic domain near the COOH terminus. Proc. Natl. Acad. Sci. U.S.A. **77**:3884–3888.
23. **Ross, S. R., S. J. Flint, and A. J. Levine.** 1980. Identification of the adenovirus early proteins and their genomic map positions. Virology **100**:419–432.
24. **Ross, S., and A. J. Levine.** 1979. The genomic map position of the adenovirus type 2 glycoprotein. Virology **99**:427–430.
25. **Storch, T. G., and J. V. Maizel, Jr.** 1980. The early proteins of the nondefective Ad2-SV40 hybrid viruses: the 19K glycoprotein is coded by Ad2 early region E3. Virology **103**:54–67.
26. **Tabas, I., and S. Kornfeld.** 1979. Purification and characterization of a rat liver Golgi α-mannosidase capable of processing asparagine-linked oligosaccharides. J. Biol. Chem. **254**:11655–11663.
27. **Wold, W. S. M., and M. Green.** 1979. Adenovirus type 2 early polypeptides immunoprecipitated by antisera to five lines of adenovirus-transformed rat cells. J. Virol. **30**:297–310.
28. **Wold, W. S. M., M. Green, and J. K. Mackey.** 1978. Methods and rationale for analysis of human tumors for nucleic acid sequences of oncogenic human DNA viruses, p. 69–161. *In* E. Busch (ed.), Methods in cancer research, vol. 15. Academic Press, Inc., New York.